

# Infrared spectroscopy studies of cyclohexene hydrogenation and dehydrogenation catalyzed by platinum nanoparticles supported on mesoporous silicate (SBA-15). Part 1: The role of particle size of Pt nanocrystals supported on SBA-15 silicate

Éva Molnár, Gyula Tasi, Zoltán Kónya, and Imre Kiricsi

*Applied and Environmental Chemistry Department, University of Szeged, Rerrich Béla tér 1, H-6720 Szeged, Hungary*

Received 15 December 2004; accepted 24 January 2005

Platinum nanoparticles were prepared from colloidal solution in the 5–16 nm range. SBA-15 mesoporous silica was impregnated with particles small enough to enter the 10 nm pores until 0.1 wt% loading was reached. Characterization of the catalysts was carried out by XRD, TEM and BET. Cyclohexene hydrogenation/dehydrogenation was monitored using a reaction cell that permitted infrared spectroscopy monitoring of the gas phase as well as the catalyst surface that was pressed in a wafer and inserted in the reactor. The surface hydroxyl groups on the mesoporous silica show shifts in the 3633–3705 cm<sup>-1</sup> range characteristic of the presence of cyclohexene, 1,3- and 1,4-cyclohexadienes. Reaction studies using 10 Torr of cyclohexene and 100 Torr of hydrogen in the 298–473 K range showed that hydrogenation occurs readily at room temperature while dehydrogenation takes place only at higher temperatures as expected. The small platinum nanoparticles carry out reactions at the highest rates while the largest size metal particles of the lowest. There is no apparent change of metal particle size during the reactions.

**KEY WORDS:** infrared spectroscopy; platinum nanoparticles.

## 1. Introduction

Supported platinum is the most widely used catalyst both in the scientific research and in industrial processes. When supported on high surface area silica, alumina or alumina silicates it is applied in oxidation and reduction reactions, decomposition leading to smaller molecules or rearrangements followed by formation of new bonds and thereby molecules. The dispersion of platinum is affected by the preparation methods (impregnation, vapor deposition, ion-exchange, incipient wetness, etc.), preparation conditions (platinum loading, surface area of support, pore size distribution in the support, decomposition of platinum precursor, dispersion of precursor on the surface, use of ultra-sound, rest fragments from decomposition of precursor, etc.), activation processes (pretreatment temperature, pretreatment atmosphere, reduction agent, acid-base properties, etc.) and the catalytic transformation itself (reconstruction of platinum surface, platinum deactivation, etc.). There are some works in the literature reporting the results of influence of several experimental parameters listed above.

In those cases where pre-prepared platinum nanoparticles were used to the production of supported catalysts, the influence of experimental conditions became somewhat simpler. As the colloid solution of platinum nanoparticles has been prepared and characterized (might be assumed that the shape and size of

the particles are known), the main parameter, strongly influencing the catalytic activity is the distribution of the particles on the support. Fast stirring or use of ultrasonic bath is generally applied while the solvent is evaporating or for obtaining rather homogeneous dispersions. For porous supports these mechanical forces become even more important, since at least part of the particles may enter the pores. To have the particles in the pores of a support – particularly in the pores of meso- or microporous silicates such as zeolites or mesoporous MCM-41 and SBA-15 type materials – platinum nanoparticles of diameter less than 1 nm or 7–8 nm are required. Synthesis of colloid solution containing such small particles has been elaborated and published [1]. The synthesis methods of zeolites and mesoporous silicates are also known [2].

The unprecedented development in surface science allowed detecting and studying the presence and the nature of various surface species generated upon interaction of various molecules with single crystal metal surfaces from UHV to atmospheric pressures [3]. As no gap exists in the operating pressures and temperatures, studies become feasible with experimental conditions being very similar to the industrial processes [4].

It has been reported several times and also reviewed that the size of the noble metal particles influences the catalytic performance [5,6]. Generally polycrystalline metal particles were prepared and studied. In the last

decades the fruit of the great effort focused on the preparation of very small crystals with well defined morphology has ripened, recipes of their synthesis have been described [7,8].

El-Sayed reported the preparation of cubic and tetrahedral Pt nanoparticles by reducing platinum ions in the presence of various capping agents [9]. Balint applied this method to prepare cubic platinum nanocrystals and after deposition on alumina tested the catalytic activity in NO reduction [10]. Excellent catalytic performance was concluded from the results obtained.

Recently Somorjai *et al.* proved that the rate of cyclohexene hydrogenation and dehydrogenation is influenced by the symmetry of the platinum single crystal faces investigated [11]. They concluded that the maximum of the turnover rate of hydrogenation appeared at lower temperature than the dehydrogenation and the maximum for hydrogenation was higher on Pt (111) while lower on Pt (100) faces than that of the dehydrogenation. The phenomenon was traced back to the difference of reaction mechanisms on the two different surfaces. This finding may serve as an excellent test reaction occurring with different rates over different crystal faces. Beside the shape, chemical and optical selectivity this novel form, the reaction rate selectivity appeared [12].

The same group reported for the first time the preparation of catalysts with well defined shaped metal (platinum, gold, silver, etc.) nanoparticles in the pore system of mesoporous silicates. In this method colloid solution of metal nanoparticles protected by organic molecules is used as template for the synthesis of SBA-15 [13] and/or MCM-41 [14] mesoporous silicates. This way novel type of catalysts composed of well shaped (cubic) metal particles and mesoporous matrix (pore size 7–8 nm) were prepared and characterized by various physico-chemical techniques.

The platinum nanoparticles may have well defined shapes like cubic, tetrahedral, cubo-octahedral, etc. The cubic particles have (100) faces while tetrahedral shape particles have (111) faces. The cubo-octahedral particles have both. In the most favored case, the platinum nanoparticles might be embedded in the pores of mesoporous silicate structures such as MCM-41 and SBA-15. The catalyst prepared in this way may mimic the catalytic processes studied in two dimensions (see above) in three dimensions.

In the following we report (i) the preparation of platinum nanocrystals of cubic shape with different size, (ii) their deposition on a silicate support, (iii) the characterization of this catalysts and (iv) their catalytic activity in various reactions investigated by IR spectroscopy. In the present paper, considered as the first publication of a series, the role of catalyst preparation and the influence of particle size of platinum particles will be discussed over catalysts of very low platinum

nanoparticle contents. The second part of the series will deal with the transformations of molecules considered to be involved in the reaction mechanism, i.e. cyclohexene, cyclohexane, 1,3-cyclohexadiene, 1,4-cyclohexadiene, benzene. The third part gives a comparison of catalytic characteristics of cubic and tetrahedral platinum particles, the role of the support mesoporous silicate and discusses the similarity of 2D and 3D catalysts.

In the experiments reported in the first two parts of papers we used catalytic amount of platinum nanoparticles (generally 0.1 wt%) supported on a high surface area (around 800 m<sup>2</sup>/g) mesoporous silicate. This very low metal/support ratio allowed us to monitor accurately the changes on the support, i.e. the wandering of final and intermediate products on the silicate surface. Consequently, we have much less chance to detect any adsorbate on the metal surfaces due to its very low surface area. Both the gas phase spectra of the reacting mixture and that of the adsorbed phase were taken with reaction time. We selected IR absorptions in the gas phase spectra suitable for identification and quantitative analysis of the reaction products. For monitoring the support the Si–OH vibration range in the 3800–3300 cm<sup>−1</sup> was investigated, while the changes in the =CH, =CH<sub>2</sub> bonds and the C=C and C–H vibrations the regions between 3200–2700 cm<sup>−1</sup> and 1600–1400 cm<sup>−1</sup> were investigated, respectively.

In this paper we report on the results obtained on supported platinum nanocrystals catalysts prepared by impregnation in which the pre-prepared platinum nanoparticle solution was used.

## 2. Experimental

The amount of platinum used for impregnation was 0.1 w% for each sample. The first sample (sample No. 1) was prepared by conventional impregnation of SBA-15 mesoporous silicate with a  $2 \times 10^{-4}$  molar solution of K<sub>2</sub>PtCl<sub>4</sub>. After evaporation of the solvent water the sample was dried at ambient temperature and stored in desiccators. The reduction of platinum ions was performed at 573 K, in hydrogen prior to IR measurements *in situ* in the IR cell. After reduction TEM images were taken from the sample. The image clearly showed (not seen), that big platinum particles were formed on the support.

For the synthesis of the colloidal solution of platinum nanoparticles,  $10^{-4}$ – $10^{-5}$  M K<sub>2</sub>PtCl<sub>4</sub> solution was prepared and the calculated amount of surface protecting compound was added while stirring. The solution was transferred into a hydrogenation flask and first nitrogen was bubbled through the solution for 20 min followed by hydrogen for 10 min. After 10 min the hydrogen stream was closed and the stirring was stopped. The crystallization of platinum was performed under static conditions at ambient temperature for 12 h in dark. The gold colored sol containing platinum nanocrystals was

stored in dark. The particle size and shape were determined from transmission electron microscopy (TEM) images. Table 1 summarizes the most important characteristics of platinum nanoparticles used in this work.

Synthesis of mesoporous silicate SBA-15 was carried out by the procedure developed by Stucky's group [15]. The product of the synthesis, a white solid matter, had high surface area and an average pore size of 8–10 nm depending on the fine parameters of the synthesis. A portion of this material was impregnated with the colloidal solution of platinum nanoparticles. The amounts mixed were as follows: 1 g of silicate and 100 ml Pt sol (0.001 g Pt) of platinum. This impregnation procedure resulted in samples containing 0.1 wt% platinum. The solvent was evaporated under vacuum at ambient temperature. The dry material was subjected to XRD measurement. The particle size of supported platinum particles was also determined by TEM.

Removal of the organic matter to make the platinum surface accessible for adsorption and reaction was performed *in situ* in the IR cell. Treatment of the self supporting wafers pressed from the samples in oxygen at 773 K followed by purging in hydrogen at 573 K. The last step of the pretreatment was the evacuation of the wafer while it was cooled to room temperature.

For the infrared spectroscopic measurements self-supporting wafers were pressed from the catalysts. Generally the thickness of the wafer was 10 mg/cm<sup>2</sup>. The wafers were placed in a sample holder and its treatment was performed in the IR cell itself. After having the wafer activated the background spectrum of the catalyst was registered. The vacuum line allowed us to load the wafer with different gases and treat the sample in various atmospheres including vacuum. For hydrogenation experiments 10 Torr of cyclohexene and 100 Torr of hydrogen were introduced into the cell. For testing the dehydrogenation of cyclohexene 10 Torr of reactant was introduced into the cell. Spectra of both the catalyst surface and the gas phase were monitored. When the wafer was in the light-path the adsorbed phase, when it was lifted up then the gas phase in the cell were investigated. Both spectra were run after each treatment step or in time under predetermined conditions.

The used catalyst samples were analyzed as well. After the catalytic run the wafers were subjected XRD and TEM tests in order to shed light on the changes of the particle size of platinum nanocrystals.

### 3. Results

#### 3.1. Characterization of the catalysts

Figure 1 shows TEM image revealing the shape and size of the platinum particles for samples as synthesized (part a) and dispersed on SBA-15 silicate (part b). Since the XRD reflections of platinum nanoparticles were very weak (due to their very low concentration), their sizes as well as their shape were estimated from TEM images. Both the mesopores and the platinum reflections were monitored but only the pore size of silicate was calculated from the first reflection of the XRD profile (it was 8.05 nm).

The BET area of the samples was determined by nitrogen adsorption at 77 K. The SBA-15 sample had a surface area of 801 m<sup>2</sup>/g.

The spectra of products of hydrogenation and dehydrogenation of cyclohexene, cyclohexane, 1,4-cyclohexadiene, 1,3-cyclohexadiene and benzene show bands well separated from each other and thereby these bands are suitable for the identification of the product composition. The spectra in the 2700–3200 cm<sup>-1</sup> and 500–1900 cm<sup>-1</sup> spectral range are seen in figure 2a. Here we indicated the bands used for the analysis of the product by arrows.

#### 3.2. Adsorption of cyclohexene and cyclohexene/hydrogen mixture on SBA-15

First, we investigated the hydrogenation and dehydrogenation of cyclohexene over SBA-15 silicate support in the absence of platinum nanoparticles. Adsorption of cyclohexene/hydrogen mixture at 373 K resulted in the shift of the OH band of the silicate to lower wavenumbers, from the original value, 3745–3538 cm<sup>-1</sup>, and new bands characteristic of CH vibrations in the 3100–2700 cm<sup>-1</sup> region appeared. In the

Table 1  
Samples, surface protecting agents, particles shapes and sizes for as prepared and used specimens

Sample	Surface protecting agent	Reduction conditions	Particle size of platinum nanoparticles (nm)	
			As prepared	After reaction
1*	None	Calcinations followed by reduction in H <sub>2</sub>	5.50 ± 2.79	4.64 ± 2.03
2	NIPA <sup>a</sup>	RT, reduction with H <sub>2</sub>	3.57 ± 0.67	3.06 ± 0.99
3	NIPA <sup>a,**</sup>	RT, reduction with H <sub>2</sub>	3.21 ± 0.74	3.07 ± 1.44

<sup>a</sup>Poly(N-isopropyl-acrylamide); <sup>b</sup>Sodium polyacrylate, \*Platinum particles of this sample were prepared by impregnation of SBA-15 with K<sub>2</sub>PtCl<sub>4</sub> followed by calcinations and reduction in H<sub>2</sub>, \*\*Used for preparation with impregnation under sonication.

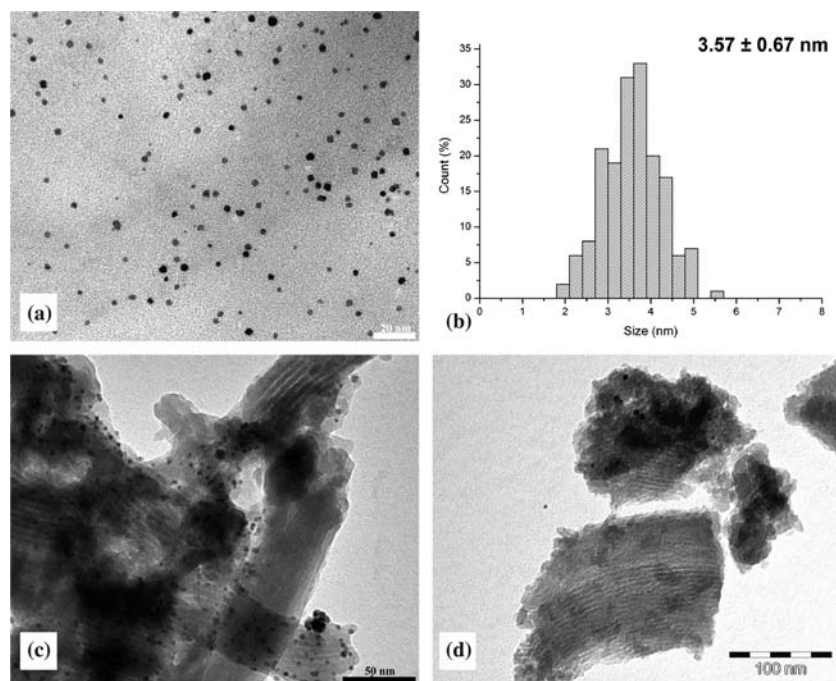


Figure 1. TEM image of Pt nanoparticles synthesized with Poly(N-isopropyl-acrylamide) capping agent (a part), the histogram of the particle size distribution (b part) after dispersed on the SBA-15 mesoporous silicate (c part), and the sample used in catalytic runs (d part).

ranges of C=C double bond vibrations weak, new absorptions developed at  $3021\text{ cm}^{-1}$  (shifted from  $3053\text{ cm}^{-1}$ ) and  $1653\text{ cm}^{-1}$  (shifted from  $1665\text{ cm}^{-1}$ ). The shifts of these bands compared to those in the gas phase spectrum of cyclohexene are 14 and  $11\text{ cm}^{-1}$ , respectively. These rather small shifts refer to weak interactions between the adsorbate and the support. The intensity of these bands did not change with time. From this follows that there is no reaction takes place under the experimental conditions over the support alone. Similar spectral changes were observed for the dehydrogenation experiments, where adsorption of cyclohexene was tested at temperature as high as 473 K. The selected difference spectra are seen in figure 3. After the adsorption experiments the cell was evacuated for 1 h. The evacuation resulted in complete disappearance of bands due to the adsorbed hydrocarbons. This indicates the complete removal of hydrocarbon molecules adsorbed on the SBA-15.

Analysis of IR spectra taken on the gas phase showed no new bands besides the bands assigned to the cyclohexene. This finding confirms the conclusions above, i.e. no reaction takes place in the absence of platinum on the support.

These experiments revealed the inactive behavior of the silicate support in hydrogenation and dehydrogenation of cyclohexene reactions. With other words, any change detected both in the gas phase spectra of reacting mixture and in the spectra of the adsorbates are due to the reaction occurring on the platinum particles. From this a second message follows as well, suggesting to use the changes in

the adsorbate spectra to monitor the transformations proceeding on the metal surface. Using this indirect monitoring we obtain detailed information on the whole heterogeneous transformation including the movement of adsorbates generated in the surface reaction.

### 3.3. Hydrogenation and dehydrogenation of cyclohexene over platinum containing catalysts

Hydrogenation and dehydrogenation over catalysts containing platinum particles of different sizes were studied in the temperature range of 298–473 K. Three samples listed in table 1 were tested. Sample No. 2 and 3 had the smallest particle size of an average  $3.57 \pm 0.67\text{ nm}$  and  $3.21 \pm 0.74\text{ nm}$ , while sample No. 5 contained the biggest ( $16.24 \pm 5.02\text{ nm}$ ) platinum particles.

Figure 4 shows the spectral changes caused by the adsorption of cyclohexene–hydrogen mixture on the specimen containing 3.57 nm platinum particles. The gas phase spectra taken at different reaction times are depicted in figure 4a. Spectrum b shows the sharp band at  $3745\text{ cm}^{-1}$  and a shallow shoulder on its low frequency leg. These bands are due partially to the structural OH groups present at different topological positions on the walls of the silicate channels. The other part of the OH groups may occupy sites on the outer surface of the mesoporous silicate. Generally, these OH groups serve as adsorption sites for any kind of hydrocarbon-type adsorbates, in our case initially the cyclohexene adsorbs on these OH groups. Upon adsorption of the cyclohexene–hydrogen mixture the

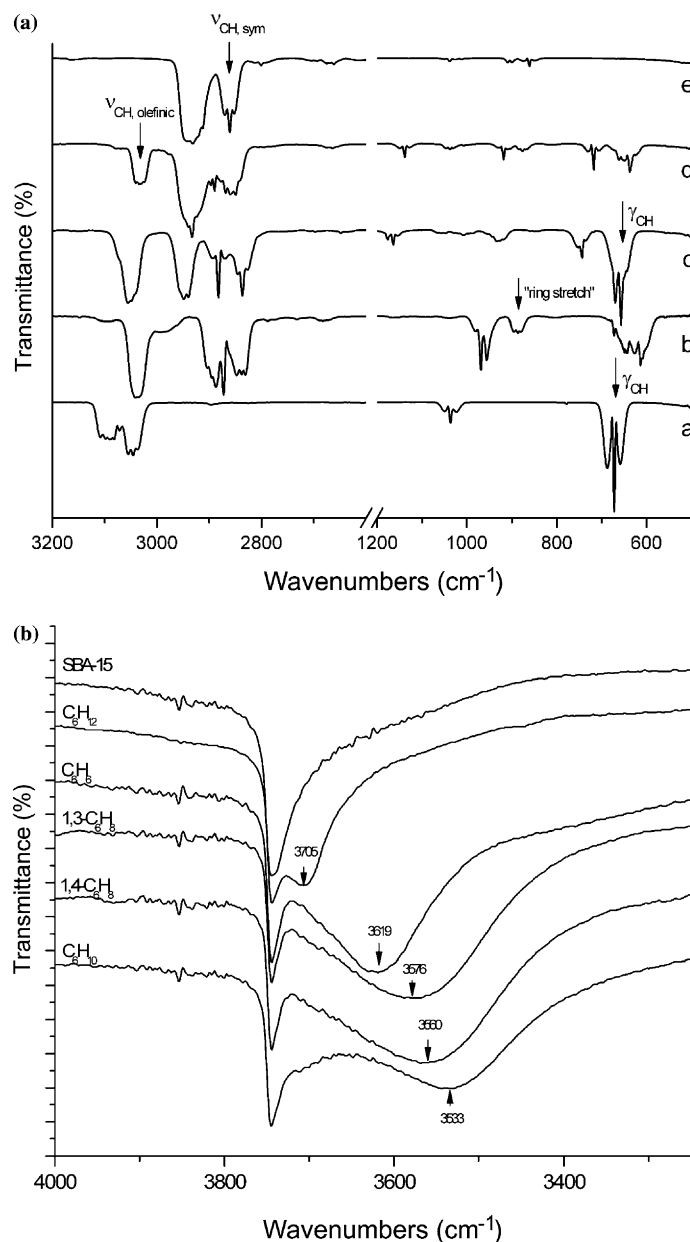


Figure 2. (a) Gas phase IR spectra of the investigated components; (a) benzene, (b) 1,4-cyclohexadiene, (c) 1,3-cyclohexadiene, (d) cyclohexene, (e) cyclohexane. Arrows indicate the bands used for analysis of the gaseous products from the references[16–19]. (b) Shifted OH bands appeared upon adsorption of the products indicated on the spectrum.

OH bands partially shifted to lower wavenumbers. A broad band centered at  $3538\text{ cm}^{-1}$  appeared after 30 min adsorption. Parallel to the appearance of this overlapped OH band new absorptions developed in the  $3100\text{--}2700\text{ cm}^{-1}$  spectral range. The band at  $3021\text{ cm}^{-1}$  is due to the double bond in the six-member ring shifting to lower wavenumbers (in the gas phase spectrum of cyclohexene it appears at  $3038\text{ cm}^{-1}$ ). The  $\text{C}=\text{C}$  stretching band at the adsorbed phase developed at  $1653\text{ cm}^{-1}$  while in the gas phase spectrum of cyclohexene this band appeared at  $1665\text{ cm}^{-1}$ . Here the shift is equal to  $12\text{ cm}^{-1}$  in accordance with that found in the high energy range. These small shifts,  $\Delta\nu = 14\text{ cm}^{-1}$  and

$12\text{ cm}^{-1}$  are identical to those measured for SBA-15 silicate without platinum. From this it follows that the cyclohexene is adsorbed on the OH groups of mesoporous silicates. This conclusion is supported by the following experimental results. After 1 h contact time the double bond character of the adsorbed species disappeared, no bands at  $3021$  and  $1653\text{ cm}^{-1}$  were detected. A characteristic change occurred in the OH region as well. The broad band flattened substantially and a new band at  $3707\text{ cm}^{-1}$  appeared besides the original  $3745\text{ cm}^{-1}$  adsorption. Upon further equilibration no change was found in the spectrum of the adsorbed species. These changes in the IR spectra indicate that

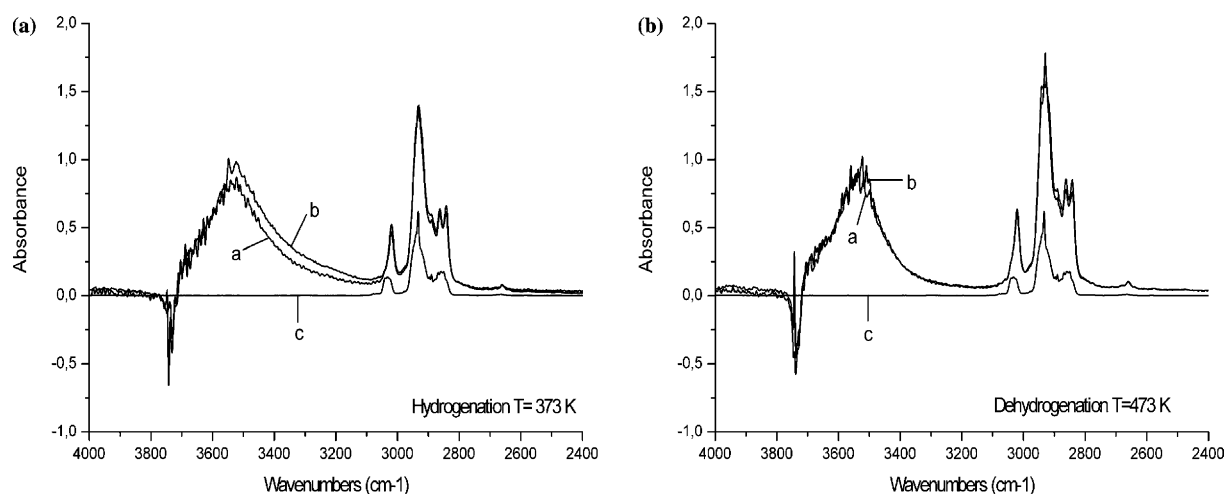


Figure 3. (a) Hydrogenation and (b) dehydrogenation of cyclohexene over SBA-15 silicate support in the absence of platinum nanoparticles; the a curves are the difference IR spectra of adsorbed cyclohexene after introducing it into the IR cell, the b curves are the difference IR spectra of adsorbed cyclohexene after heat treatment, c curves are the original gas phase spectra of cyclohexene.

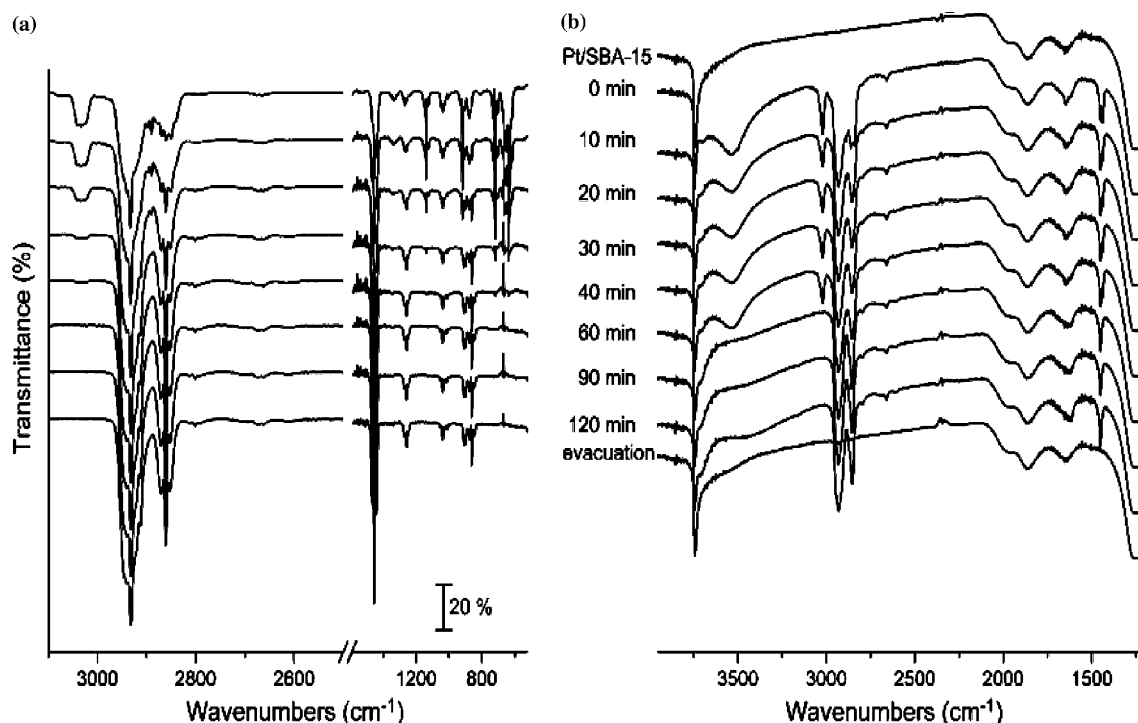


Figure 4. Spectral changes in the gas phase (a) and in the adsorbed phase (b) caused by the adsorption of cyclohexene–hydrogen mixture on the specimen containing 3.57 nm platinum particles.

cyclohexene adsorbed on the OH groups of silicate moves to the platinum surface and transform there. The products of the hydrogenation occupy the same adsorption sites, moving from the platinum surface to the support and cover the OH sites. The new band observed at  $3707\text{ cm}^{-1}$  is attributed to the OH vibrations perturbed by the adsorbed cyclohexane on the basis of the spectra shown in figure 2B, where the spectrum of cyclohexane adsorbed on SBA-15 containing no platinum is shown.

Simultaneously, the changes in the gaseous spectra of hydrocarbons in the IR cell were as follows. The bands due to the double bond in the starting cyclohexene disappeared and the spectrum became identical to that of the cyclohexane being the product of hydrogenation reaction.

The bonding of the product cyclohexane to the platinum nanoparticles and/or to the OH groups of the support should be weak since the original spectrum of adsorbate free adsorbent, the Pt supported SBA-15 was

recovered after evacuating the system at ambient temperature for 1 h.

The hydrogenation reaction was investigated at 298, 323, 353 and 373 K. Using the integrated intensities of absorption bands (marked with arrows in figure 2A) of spectra taken of the gas phase after equilibration at 323 K, at different reaction times an approximate kinetic feature of the reaction could be concluded. Figure 5 shows the kinetic curves determined from the integrated absorption of the cyclohexene band (band at  $3035\text{ cm}^{-1}$ ). The following informations were learned from these graphs. The first is that the rate of transformation seems to be influenced by the particle size at 323 K. The fastest rate was established for the smallest particles whiles the lowest for the biggest platinum particles. However, this feature should be regarded with caution, since the gas phase in the IR cell was not stirred and the system was static, the influence of diffusion cannot be disregarded.

The kinetic curves for hydrogenation and dehydrogenation reactions are depicted in figure 5.

The hydrogenation reaction of cyclohexene was investigated at different temperatures. For these experiments the IR spectra of the gas phase were taken after treating the wafer in the presence of substrate at 298, 323 and 353 K. On the basis of the data obtained in the course of these studies the approximate kinetic curves of the transformation at different temperatures have been determined and are depicted in figure 6.

Dehydrogenation of cyclohexene over platinum nanoparticles supported on SBA-15 took place at much higher temperature than the hydrogenation. When the pretreated wafer was loaded with 10 Torr of cyclohexene at 473 K immediate development of CH bands was observed as can be seen in figure 7.

Here again the adsorption took place on the OH groups as was indicated by the shift of the OH bands to lower wavenumbers. After 30 min reaction time the

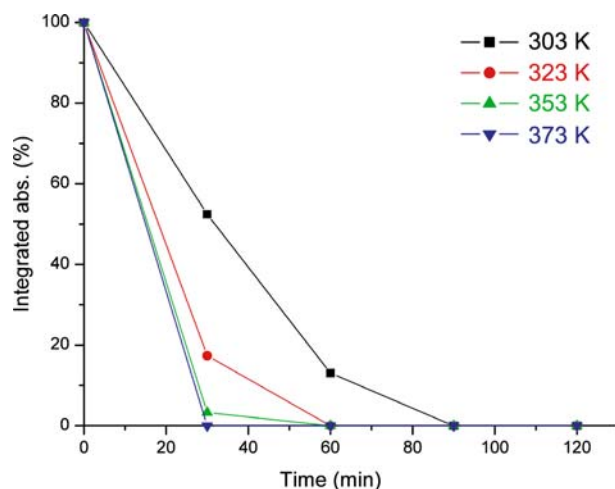


Figure 6. Kinetic curves of hydrogenation reaction of cyclohexene at different temperatures on sample No. 2.

initial changes are seen in the spectrum. The OH bands became more structured, new bands appeared in the  $\text{CH}_2$ ,  $\text{CH}_3$  region and some new bands around  $1500\text{ cm}^{-1}$  get to develop. Upon treatment the wafer for 1.5 h at the same temperature the decrease of the intensity of the double bond, development and growth of new bands at  $3069$  and  $3090\text{ cm}^{-1}$  was seen. Parallel to this the split of the band at  $1448\text{ cm}^{-1}$  occurred. Upon 2 h reaction time a new band appeared at  $1477\text{ cm}^{-1}$ . Simultaneously the bands at  $3069$  and  $3090\text{ cm}^{-1}$  increased in intensities. In the OH region a band centered at  $3619\text{ cm}^{-1}$  became the most intense. Longer reaction time did not cause further change in the intensities of absorptions. These spectral changes show the dehydrogenation of cyclohexene to benzene. The bands at  $1477$ ,  $3069$  and  $3090\text{ cm}^{-1}$  are attributed to the benzene adsorbed on the catalyst. Two experimental evidences support this assignment.

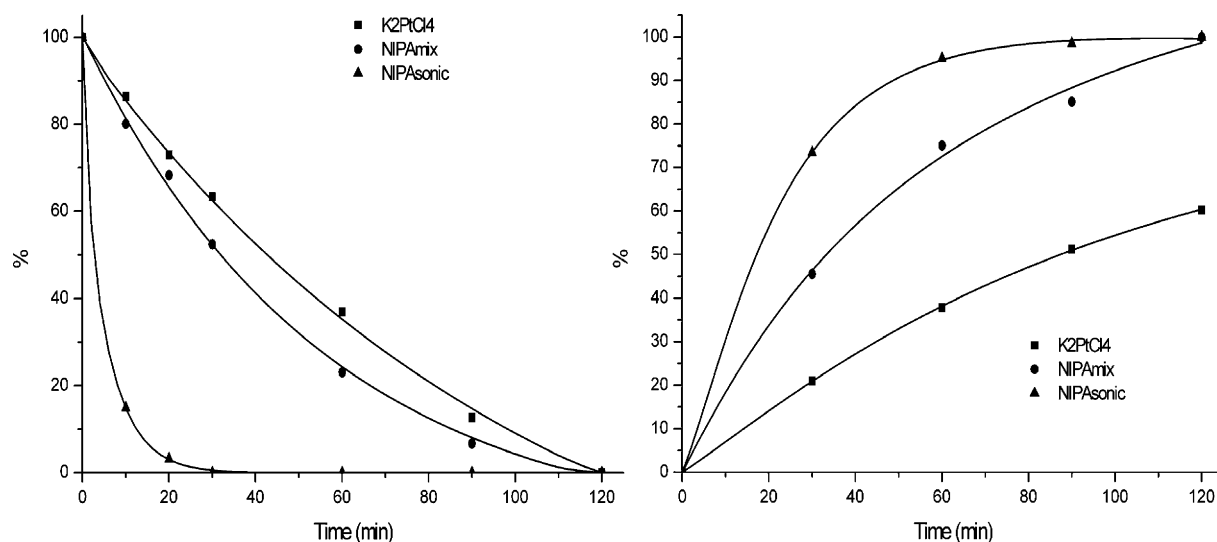


Figure 5. Kinetic curves of hydrogenation of cyclohexene at 298 K on samples No. 1 (■), 2 (●) and 3 (▲).

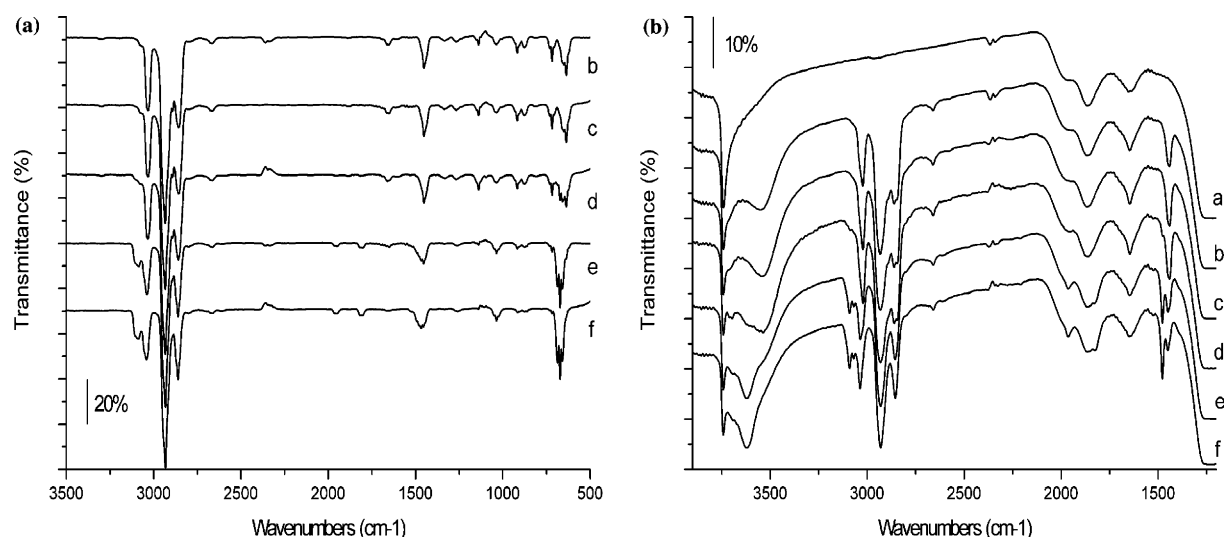


Figure 7. Dehydrogenation of cyclohexene (spectrum b on figure (a)) over platinum nanoparticles supported on SBA-15 (spectrum a on figure (b)). IR spectrums were taken at 30 (c), 60 (d), 90 (e) and 120 min (f) (sample No.1 – Pt size:  $3.57 \pm 0.67$  nm).

The spectrum of adsorbed benzene on SBA-15 containing no platinum shows this band (see figure 2B). Further support can be found to this assignment in zeolite chemistry. The band at  $3619\text{ cm}^{-1}$  generally appeared when benzene was adsorbed in zeolites containing SiOH groups. In these cases a  $\Delta\nu > 100\text{ cm}^{-1}$  shift of OH band was found [20]. Upon evacuation of the IR cell at ambient temperature the bands disappeared and we got back the base spectrum of the sample.

Analysis of the kinetic behavior of dehydrogenation reaction on catalysts showed that sample No. 1 exhibited negligible activity; No. 2 had low activity, while No. 3 was active. These results show that the activity order of the catalysts decreased with increasing the size of the platinum particles. This trend is identical to that obtained for hydrogenation reaction. An additional observation was the temperature difference between the hydrogenation and dehydrogenation reaction. The dehydrogenation took place around 473 K while the hydrogenation proceeded already at ambient temperature.

As far as the agglomeration of platinum nanoparticles is concerned, in each case a TEM measurement was carried out to monitor the size of the particles. We found that no significant agglomeration took place, i.e. the size of the particles remained unchanged within the error of the measurement.

#### 4. Conclusions

Different sizes of platinum nanoparticles were prepared in aqueous solution using organic surface protecting agents. SBA-15 mesoporous silicate was synthesized applying a conventional procedure. This silicate was impregnated with the colloid solution of platinum nanoparticles.

Simultaneous measurement of the spectrum of surface species and the gas phase products allowed us to investigate the hydrogenation and dehydrogenation of cyclohexene over catalysts containing platinum nanoparticles of different size.

We found that the hydrogenation reaction took place already at ambient temperature while dehydrogenation requires much higher temperature.

The further conclusion we drawn is that we suggest to compare the action of metal particles of relatively narrow particle size distributions. The nanometer sized particles, their size should be lower than 10 nm cannot be compared to much bigger platinum clusters since in the later case a polycrystalline phase is expected with completely different catalytic behavior. We suggest comparing the catalytic activity only for those catalysts in which the platinum particles have a size less than 20 nm, since for particle sizes above this measure several factors are influencing the catalyst performance.

We calculated the apparent first order rate constants for hydrogenation reaction occurring on platinum nanoparticles of different size and for the smallest particle size at different temperature.

There was no significant change in the particle size of platinum nanocrystals caused by the reaction. Their size fell into the same size range before and after the reaction.

#### Acknowledgments

Authors thank the support of the OTKA 048978 and the MTA-OTKA-NSF project (No: 30.008./24/2003). KZ acknowledges the financial support of the MTA Bolyai Janos fellowship.



## References

- [1] T.S. Ahmadi, Z.L. Wang, T.C. Green, A. Henglein and M.A. El-Sayed, *Science* 272 (1996) 1924.
- [2] J.B. Nagy, P. Bodart, I. Hannus and I. Kiricsi, *Synthesis characterization and use of zeolitic microporous materials* (DecaGen Ltd, Szeged, Hungary, 1998).
- [3] G.C. Bond, *Heterogenous Catalysis: Principles and Applications*. (Oxford University Press, 1987).
- [4] P. Chen, S. Westerberg, K.Y. Kung, J. Zhu, J. Grunes and G.A. Somorjai, *Appl. Catal. A: Gen.* 229 (2002) 147.
- [5] A. Wieckowski, E.R. Savinova and C.G. Vayenas, *Catalysis and Electrocatalysis at Nanoparticle Surfaces* (Marcel Dekker, New York, 2003).
- [6] W. Tu, H. Liu and Y. Tang, *J. Mol. Catal. A: Chem.* 159 (2000) 115.
- [7] A. Miyazaki, I. Balint and Y. Nakano, *J. Nanoparticle Res.* 5 (2003) 69.
- [8] T. Teranishi, R. Kurita and M. Miyake, *J. Inorg. Organomet. P.* 10 (2000) 145.
- [9] R. Narayanan and M.A. El-Sayed, *Nano Lett.* 4 (2004) 1343.
- [10] I. Balint, A. Miyazaki and K. Aika, *Appl. Catal. B: Env.* 37 (2002) 217.
- [11] K.R. McCrea and G.A. Somorjai, *J. Mol. Catal. A: Chem.* 163 (2000) 43.
- [12] X. Su, K.Y. Kung, J. Lahtinen, Y.R. Shen and G.A. Somorjai, *J. Mol. Catal. A: Chem.* 141 (1999) 9.
- [13] Z. Kónya, V.F. Puentes, I. Kiricsi, J. Zhu, A.P. Alivisatos and G.A. Somorjai, *Catal. Lett.* 81(3–4) (2002) 137.
- [14] Z. Kónya, V.F. Puentes, I. Kiricsi, J. Zhu, J.W. Ager, M.K. Ko, H. Frei, P. Alivisatos and G.A. Somorjai, *Chem. Mater.* 15 (2003) 1242.
- [15] D. Zhao, J. Feng, Q. Huo, N. Melosh, G.H. Fredrickson, B.F. Chmelka and G.D. Stucky, *Science* 279 (1998) 548.
- [16] L.J. Shorthouse, Y. Jugnet and J.C. Bertolini, *Catal. Today* 70 (2001) 33.
- [17] S.W. Lee, L.N. Nelen, H. Ihm, T. Scoggins and C.M. Greenlief, *Surf. Sci.* 410 (1998) L773.
- [18] V.M. Bermudez, *Surf. Sci.* 540 (2003) 255.
- [19] C.L.A. Lamont, M. Borbach, R. Martin, P. Gardner, T.S. Jones, H. Conrad and A.M. Bradshaw, *Surf. Sci.* 374 (1997) 215.
- [20] I. Kiricsi, C. Flego, G. Pazzuconi, W.O. Parker Jr., R. Millini, C. Perego and G. Bellussi, *J. Phys. Chem.* 98 (1994) 4627.